ORIGINAL RESEARCH ARTICLE

Presence of Cx43 in extracellular vesicles reduces the cardiotoxicity of the anti-tumour therapeutic approach with doxorubicin

Tania Martins-Marques[1,2], Maria Joao Pinho[1,2], Monica Zuzarte[1,2], Carla Oliveira[3,4,5], Paulo Pereira[6], Joost P. G. Sluijter[7,8], Celia Gomes[2,9,10] and Henrique Girao[1,2]*

[1]Institute of Biomedical Imaging and Life Sciences (IBILI), Faculty of Medicine, University of Coimbra, Coimbra, Portugal; [2]CNC.IBILI, University of Coimbra, Coimbra, Portugal; [3]Expression Regulation in Cancer Group, Instituto de Investigação e Inovação em Saúde (i3S), Porto, Portugal; [4]Institute of Molecular Pathology and Immunology of the University of Porto (IPATIMUP), Porto, Portugal; [5]Department of Pathology and Oncology, Faculty of Medicine, University of Porto, Porto, Portugal; [6]Chronic Diseases Research Center (CEDOC), NOVA Medical School, Faculdade de Ciências Médicas, Universidade NOVA de Lisboa, Lisboa, Portugal; [7]Department of Cardiology, Division of Heart & Lungs, University Medical Center Utrecht, Utrecht, The Netherlands; [8]Interuniversity Cardiology Institute Netherlands (ICIN), Utrecht, The Netherlands; [9]Laboratory of Pharmacology and Experimental Therapeutics, IBILI, Faculty of Medicine, University of Coimbra, Coimbra, Portugal; [10]Center of Investigation in Environment, Genetics and Oncobiology (CIMAGO), Faculty of Medicine, University of Coimbra, Coimbra, Portugal

Extracellular vesicles (EVs) are major conveyors of biological information, mediating local and systemic cell-to-cell communication under physiological and pathological conditions. These endogenous vesicles have been recognized as prominent drug delivery vehicles of several therapeutic cargoes, including doxorubicin (dox), presenting major advantages over the classical approaches. Although dox is one of the most effective anti-tumour agents in the clinical practice, its use is very often hindered by its consequent dramatic cardiotoxicity. Despite significant advances witnessed in the past few years, more comprehensive studies, supporting the therapeutic efficacy of EVs, with decreased side effects, are still scarce. The main objective of this study was to evaluate the role of the gap junction protein connexin43 (Cx43) in mediating the release of EV content into tumour cells. Moreover, we investigated whether Cx43 improves the efficiency of dox-based anti-tumour treatment, with a concomitant decrease of cardiotoxicity. In the present report, we demonstrate that the presence of Cx43 in EVs increases the release of luciferin from EVs into tumour cells *in vitro* and *in vivo*. In addition, using cell-based approaches and a subcutaneous mouse tumour model, we show that the anti-tumour effect of dox incorporated into EVs is similar to the administration of the free drug, regardless the presence of Cx43. Strikingly, we demonstrate that the presence of Cx43 in dox-loaded EVs reduces the cardiotoxicity of the drug. Altogether, these results bring new insights into the concrete potential of EVs as therapeutic vehicles and open new avenues toward the development of strategies that help to reduce unwanted side effects.

Keywords: *extracellular vesicles*; *drug delivery*; *cancer*; *cardioprotection*; *intercellular communication*

Extracellular vesicles (EVs), including exosomes and microvesicles, are nano-sized particles that can be released by virtually every cell type into the extracellular milieu (1–3). Hence, EVs are found in several body fluids including saliva, urine, malignant ascites, and blood, and they are considered important tools for diagnosis and therapy (3). Because EVs are able to cross stringent biological barriers and remain

in circulation without eliciting immune responses, these vesicles have emerged as excellent candidates for drug delivery (4,5). Importantly, the therapeutic value of EVs largely depends upon an efficient uptake and intracellular processing of deliverable material. Although a few different models have been proposed to depict the mechanisms underlying EV–cell interaction, the most robust evidence pointed to endocytosis or membrane fusion of EVs within target cells (3,6). Recently, we proposed an additional mode of communication, involving connexin43 (Cx43)-containing channels. Results from our lab demonstrated that the gap junction (GJ) protein Cx43, embedded in EV membranes, forms a channel that facilitates the release of intravesicle content into recipient cells, likely playing important functions on selective EV targeting, increased cargo delivery, or both (7).

Mounting lines of evidence established the therapeutic potential of endogenous membrane-enclosed vesicles, mostly focused on inflammation and cancer. For example, curcumin-loaded exosomes were found to confer protection in mice models of lipopolysaccharide-induced sepsis, whereas intratumoural delivery of microvesicles carrying the cytosine deaminase mRNA and protein, in combination with systemic delivery of a pro-drug, leads to reduced growth of schwannoma xenografts *in vivo* (8,9).

Given that cancer cells express a myriad of membrane receptors that can confer targeting selectivity, EV homing has been attempted through the use of engineered vesicles with surface-targeting peptides (4,10,11). This enhanced tropism is particularly important to mitigate the side effects of cytotoxic compounds. For example, doxorubicin (dox) is among the most effective chemotherapeutic agents used in the clinical practice, with indications for a wide variety of cancers. Nevertheless, its use has been limited by the high incidence of acute cardiotoxicity that arises in about 11% of the patients (12). Consequently, EVs or liposomal formulations of dox have been considered as valuable therapeutic alternatives to decrease toxicity to non-target organs (13,14). Tian et al. demonstrated that exosomes with surface expression of the internalizing-RGD peptide (Arg-Gly-Asp); amino acid sequence CRGDK/RGPD/EC peptide, exogenously loaded with dox, display enhanced tropism to breast cancer xenografts and increased therapeutic efficiency (10). Given its potential, additional studies are required to deeply demonstrate the efficacy of EVs as dox-carrying agents.

Although it is known that initial stages of tumour growth involve a downregulation of Cx43, further dissemination and colonization of malignant cells require the presence of Cx43 (15,16). Therefore, we hypothesized that Cx43 can constitute a target to direct therapeutic vehicles within specific stages of tumour development. In the present work, we investigated whether the presence of Cx43 improves the therapeutic potential of EVs as carriers of dox, with a concomitant reduction of cardiotoxicity in a subcutaneous breast cancer mouse model.

Materials and methods

Cell culture and animal models

Human embryonic kidney (HEK)-293 and 4T1^{luc2} (Perkin Elmer) cell lines were maintained in Dulbecco's modified Eagle's medium (DMEM) (Life Technologies), supplemented with 10% foetal bovine serum (FBS, Gibco), penicillin/streptomycin (100 U/ml:100 µg/ml) and 1% GlutaMax (Life Technologies). Animals were handled according to European Union guidelines (86/609/EEC), with approval of the Ethics Committee, Faculty of Medicine, University of Coimbra. The tumour model was established by subcutaneous injection of 0.5×10^6 murine breast 4T1^{luc2} cells in opposite flanks of 12-week-old female Swiss nude mice (Charles River) (17,18). EVs loaded with luciferin and dox were resuspended in phosphate-buffered saline (PBS) (10 µg of EVs/20 µl of PBS) and intratumourally (i.t.) injected. Tumour growth was monitored 5, 8 and 11 days post-inoculation by bioluminescence imaging (BLI) with an IVIS Lumina II XR (PerkinElmer), 8 min after intra-peritoneal (i.p.) injection of D-luciferin (150 mg/kg), with animals under anaesthesia (100 mg/kg ketamine and 2.5% chlorpromazine). Images were analysed with Living Imaging 4.10 (Caliper Life Sciences SA) (19). A region of interest (ROI) was drawn around the tumour for bioluminescence quantification. Tumour volumes were assessed with a manual caliper and calculated with the formula (length $\times$ width^2)/2. Experiments were ended before tumours reached a 2 cm^3 volume endpoint. Animals were sacrificed, tumours and hearts were harvested, and then they were embedded in optimum cutting temperature (OCT) matrix (Tissue-Tek) for cryosectioning, or snap-frozen in liquid nitrogen for biochemical studies, before storage at $-80°$C.

EV purification

HEK-293 cells expressing Cx43 or not (HEK-293^{Cx43+} and HEK-293^{Cx43-}) (7) were cultured in EV-depleted medium, prepared by ultracentrifugation of 50% FBS (120,000 g, 16 h). Supernatants were diluted to a final concentration of 10% FBS in DMEM. After 48 h, conditioned medium was collected for EV isolation by differential centrifugation at 4°C, starting with 10 min at 300 g, and 20 min at 16,500 g. Supernatants were filtered (0.22 µm filter units, cellulose acetate) and ultracentrifuged (120,000 g, 70 min) (20). Pellets were resuspended in PBS and immediately used for EV loading. On average, 0.5 µg of purified EVs was obtained per 1 million cells. Transmission electron microscopy (TEM) characterization of EVs was performed as described previously (7).

EV loading

Five micrograms of EVs was incubated with 150 µM 1-(4,5-dimethoxy-2-nitrophenyl)ethyl ester (DMNPE)-caged-D-luciferin for 1 h, at 37°C, protected from light. Luciferin was released from the DMNPE group by UV-B (365 nm) photolysis (5 min, on ice) using an UV transilluminator (7,21).

Non-incorporated luciferin was removed using Exosome Spin Columns (Life Technologies). Luciferin-loaded EVs were added to 4T1^{luc2} seeded in 96-well plates, or injected i.t. into mice, followed by BLI. Ten micrograms of EVs was mixed with 100 μg of dox (DOXO-cell®) in PBS supplemented with 5 mM EDTA, and then the mixture was electroporated at 35 V and 150 μF using 0.4 cm cuvettes in a Gene Pulser II electroporator (Bio-Rad) (10,21). Empty EVs were also electroporated. Non-incorporated dox was washed out with PBS by using ultracentrifugation (120,000 g, 70 min). Loaded dox was quantified by fluorescence detection in a Biotek Synergy HT microplate reader (emission, 594 nm; excitation, 480 nm) with Gen 5 software (BioTek). Fluorescence readings were compared with a standard curve of free dox. On average, yield of dox encapsulation was 10%.

Determination of cell viability, proliferation, motility and colony formation *in vitro*

4T1^{luc2} cells were treated with 2 μM free dox or dox-loaded EVs for 24 h, when appropriate. Metabolic activity, through the 3-(4,5-dimethylthiazol-2-yl)-2.5-diphenyl tetrazolium bromide (MTT, Sigma) assay (17), and cell viability, by Trypan blue exclusion or flow cytometry, after propidium iodide (PI) staining, were performed as described previously (22,23). Cell proliferation was assessed by 5-bromo-2′-deoxyuridine (BrdU) incorporation according to the manufacturer's instructions (Roche Diagnostics). Where indicated, cells were treated with 0.25 mg/ml gap26 (Caslo) for 1 h. Staining of ki-67–positive cells was performed by immunofluorescence (1:100, AB16667, Abcam) (24). Images were obtained using an Axio Observer.Z1 inverted microscope (Zeiss) and analysed with ImageJ (National Institutes of Health). Cell cycle analysis was performed by flow cytometry, after PI/RNase staining (Immunostep) (25). Cell motility was analysed by time-lapse video microscopy (6 h, 3 min acquisition interval, using an Axio Observer.Z1 inverted microscope), with the cells under an atmosphere of 5% CO_2 at 37°C. Manual cell tracking analysis was performed with ImageJ (26). For colony formation assay, cells were treated for 48 h, as indicated, after which medium was replaced by a drug-free medium, and cells were allowed to grow for 7 days. At the end of the experiment, cells were fixed and stained with crystal violet (Sigma-Aldrich) (27). Microscopy images were obtained using an Axio Observer.Z1 inverted microscope.

Western blot

Cell and tissue lysates were prepared as described previously (28). EV pellets were lysed in a non-reducing loading buffer. Primary antibodies against CD63 (1:500, AB0047, Sicgen), CD81 (1:250, Sc9158, Santa Cruz Biotechnology), Cx43 (1:2,500, AB0016, Sicgen), Calnexin (1:5,000, AB0041, Sicgen), phosphorylated and total p44/42 (1:500, 4377S and 9102, Cell Signaling Technology),

Bax (1:250, Sc6236, Santa Cruz Biotechnology) and Bcl2 (1:250, Sc7382, Santa Cruz Biotechnology) were used, followed by incubation with horseradish peroxidase–conjugated secondary antibodies (1:10,000, Bio-Rad). Images were visualized in a VersaDoc system (Bio-Rad). Densitometric quantification was performed in unsaturated images using ImageJ.

Immunofluorescence staining and histology

Immunofluorescence staining of tissue samples (5 μm cryosections) was carried out as described previously (29). Fixation was performed with acetone and blocking with 2.5% bovine serum albumin. Primary antibodies against cyclooxygenase (COX)-2 (1:100, ab15191, Abcam), Hsp27 (1:50, SPA-803, Stressgen) and Cx43 (1:250, AB0016, Sicgen) were used. Images were collected with an Axio Observer.Z1 inverted microscope. For haematoxylin and eosin (HE) and Sirius red (0.1% in saturated aqueous picric acid) staining, slices were fixed in 4% paraformaldehyde (30). Images were collected with an AxioLab.A1 microscope (Zeiss). Quantitative analysis (at least 10 randomly chosen fields) was performed using ImageJ, including measure of transverse diameter of the myocytes cut at the level of the nucleus and area of fibrosis.

Statistical analysis

Data were analysed with Prism 7, version 7.0a (GraphPad Software, Inc.). Statistical significance was assessed by Student's t-test or Kruskal–Wallis test, where appropriate. Experimental data were presented as scatterplots plus mean (31), or as mean ± standard error of the mean, where applicable.

Results

Cx43 mediates the communication between EVs and tumour cells

In the present work, we hypothesized that Cx43 facilitates the direct transfer of EV cargo, including cytotoxic drugs, into tumour cells, thus contributing to improve the therapeutic potential of EVs. First, we demonstrated that our preparations of EVs, obtained from HEK-293 cells, containing or not Cx43, EV$^{Cx43 +}$ or EV$^{Cx43 -}$ (7,32), are positive for canonical EV markers, such as the tetraspanins CD63 and CD81 (Fig. 1a), and present typical size and morphology (Fig. 1b). In addition, the presence of higher molecular weight forms of Cx43, in non-reducing WB, suggests that EV-Cx43 is assembled into hexameric structures (Fig. 1a). This is in accordance with our previous report, wherein we characterized in great detail Cx43-containing EVs (7).

To evaluate whether Cx43 enhances the EV uptake by tumour cells, EV$^{Cx43 +}$ or EV$^{Cx43 -}$ were exogenously loaded with luciferin, after which they were added to 4T1^{luc2} tumour cells, overexpressing the firefly luciferase and endogenously expressing Cx43. We observed that
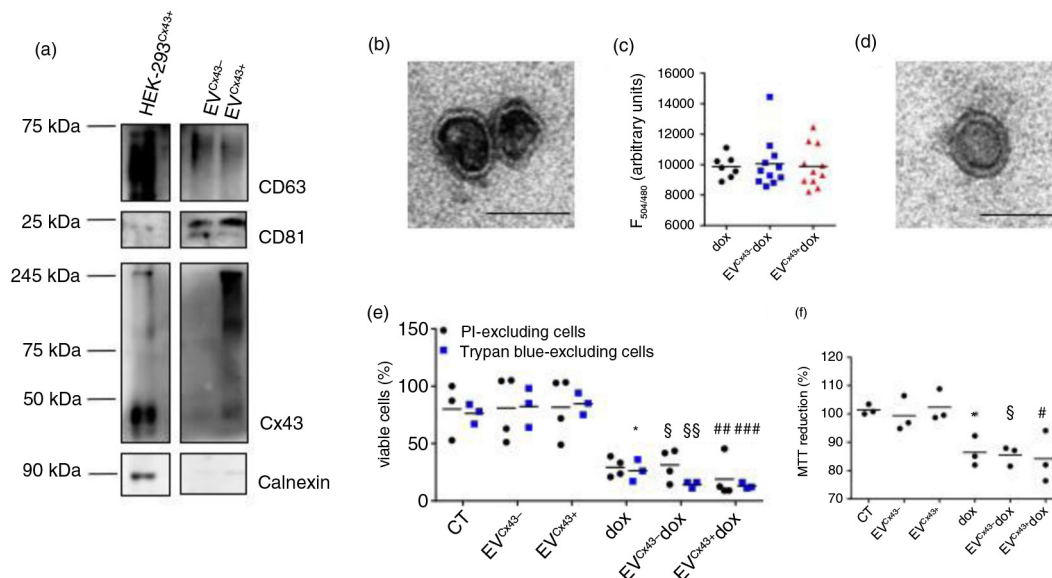
Fig. 1. EVs loaded with dox decrease the viability of tumour cells *in vitro*. (a) Characterization of EVs produced by HEK-293 cells expressing or not Cx43 (EV^{Cx43+} or EV^{Cx43-}) was performed by WB under non-reducing conditions. The presence of EV markers CD63 and CD81 was analysed. Calnexin was used as control for cell debris contamination. Equal amounts of protein (10 µg) from total cellular extracts from HEK-293^{Cx43+} were used as control. (b) Representative TEM image of EV^{Cx43+}. Scale bars, 100 nm. (c) Ten micrograms of EV^{Cx43-} or EV^{Cx43+} was loaded with 100 µg dox by electroporation; not incorporated dox was washed out with PBS by ultracentrifugation. Values of EV-loaded dox (~10% EV pellet) were quantified by fluorescence detection (emission, 594 nm; excitation, 480 nm) and are depicted in the graph. Fluorescence reading of similar amounts of free dox was used as control (n = 10). (d) Representative TEM image of EV^{Cx43+} dox after electroporation. Scale bars, 80 nm. (e) 4T1^{luc2} cells were treated with either 2 µM free dox or dox loaded into EVs containing or not Cx43 (EV^{Cx43+} dox and EV^{Cx43-} dox) for 24 h. Equal amounts of EV^{Cx43+} or EV^{Cx43-} were used for dox loading, and vehicle-treated cells were used as controls. Cell viability was assessed by flow cytometry analysis of propidium iodide (PI) exclusion and by counting the number of Trypan blue–excluding cells. Number of viable cells is represented as percentage of total cells (n = 3, $*p < 0.05$ vs. CT, $^{§}p < 0.05$, $^{§§}p < 0.01$ vs. EV^{Cx43-}, $^{##}p < 0.01$ $^{###}p < 0.001$ vs. EV^{Cx43+}). (f) Metabolic activity was assessed by MTT reduction (n = 3, $*p < 0.05$ vs. CT, $^{§}p < 0.05$ vs. EV^{Cx43-}, $^{#}p < 0.05$ vs. EV^{Cx43+}).

the light emitted by 4T1^{luc2} cells incubated with intact EV^{Cx43+} is 1.7-fold higher, compared with that of cells exposed to EV^{Cx43-} (Supplementary Fig. 1a), an effect that is maintained in a dose-dependent manner (Supplementary Fig. 1b). The levels of light emission after EV lysis are similar in both populations of vesicles (Supplementary Fig. 1a), suggesting that the same amount of luciferin was loaded into EVs, regardless the presence of Cx43.

EVs loaded with dox are cytotoxic for tumour cells in vitro

Then, we tested the efficiency of Cx43-containing EVs in the delivery of dox to tumour cells. First, by fluorimetric analysis, we demonstrated that a similar amount of dox was incorporated into EV^{Cx43+} and EV^{Cx43-} (Fig. 1c). Also, we showed that the electroporation procedure did not compromise EV integrity (Fig. 1d), nor EV-Cx43 levels (Supplementary Fig. 2a). To compare the cytotoxicity of dox, equal amounts of dox (2 µM), either free or loaded into EV^{Cx43+} or EV^{Cx43-} (EV^{Cx43+} dox or EV^{Cx43-} dox), were added to recipient 4T1^{luc2} cells for 24 h. As control, empty EVs were used. Results in Fig. 1e show a dramatic decrease in cell viability after 24 h treatment with free dox,

an effect that was further enhanced in cells treated with EV^{Cx43+} dox, compared with their respective vehicle-treated cells. However, no significant differences were found between free dox and dox-loaded EVs, neither among EV^{Cx43+} dox nor EV^{Cx43-} dox treatments. In addition, we demonstrated that treatment with dox equally reduced the metabolic activity of tumour cells (Fig. 1f), regardless the delivery vehicle, in a dose-dependent manner (Supplementary Fig. 2b). The addition of empty EVs had no significant alterations upon cell viability or metabolic activity.

EVs loaded with dox impair tumour cell proliferation and motility in vitro

Next, we evaluated the effect of EV-dox in counteracting the abnormal proliferation of tumour cells, by using different complementary approaches (33). Results on Fig. 2a show that the percentage of ki-67–positive cells is lower in the presence of EV-dox than the free drug. Regarding the BrdU incorporation, a more pronounced decrease was observed in cells treated with EV^{Cx43+} dox (Fig. 2b). This was further corroborated by the cell cycle analysis, where treatment with EV^{Cx43+} dox induced a cell cycle arrest in G2/M phase, accompanied by a decrease
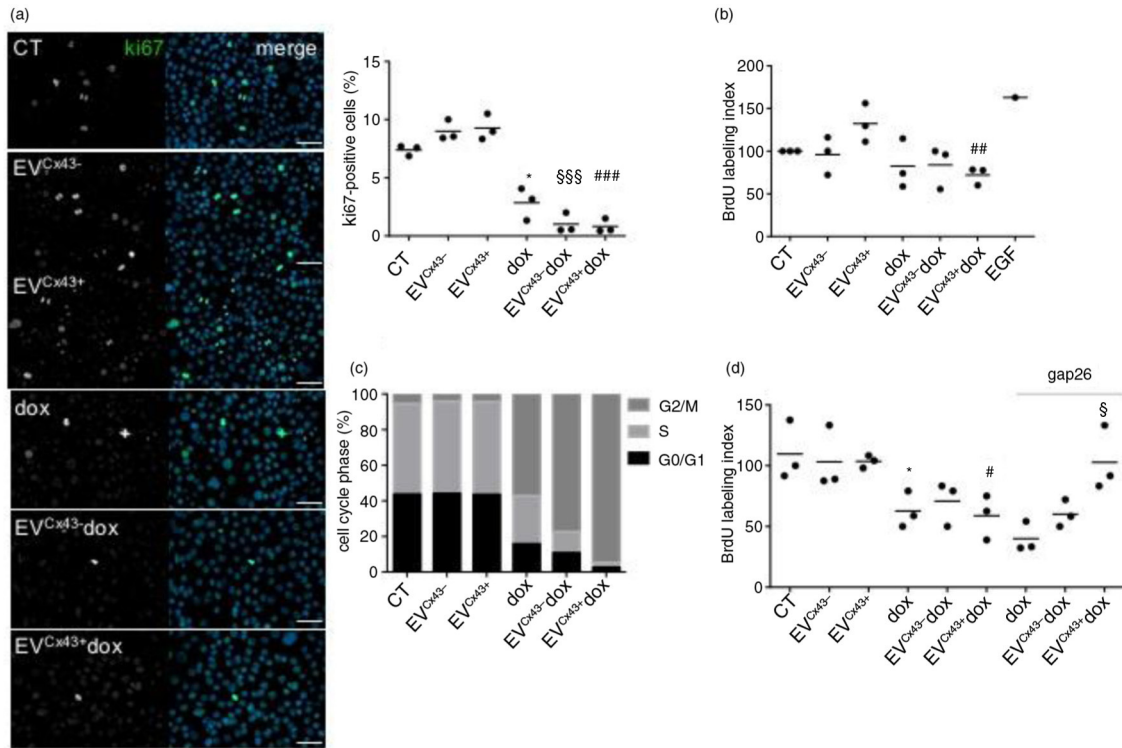
Fig. 2. EVs loaded with dox impair tumour cell proliferation *in vitro*. 4T1^{luc2} cells were treated with 2 µM free dox, EV$^{Cx43 +}$ dox, EV$^{Cx43 -}$ dox or vehicles, for 24 h. (a) Representative images of ki-67 immunostaining (green). Nuclei were stained with 4,6-diamidino-2-phenylindole (Dapi). Scale bars, 50 µm. Percentage of ki-67 (per total nuclei) is plotted in the graph (n = 3, *p < 0.05 vs. CT, §§§p < 0.001 vs. EV$^{Cx43 -}$, $^{###}$p < 0.001 vs. EV$^{Cx43 +}$). (b) Cell proliferation was assessed by the BrdU assay. Treatment with epidermal growth factor (100 ng/ml, 24 h) was performed as positive control. Percentage of BrdU incorporation is plotted on the graph (n = 3, $^{##}$p < 0.01 vs. EV$^{Cx43 +}$). (c) Cell cycle analysis was performed by flow cytometry, using PI (n = 3). (d) 4T1^{luc2} cells were treated with 2 µM free dox, EV$^{Cx43 +}$ dox, EV$^{Cx43 -}$ dox or vehicles, for 1 h. A Cx43-mimetic peptide (gap26, 0.25 mg/ml) was used, where indicated. Fresh media was added and the cells cultured for an additional 23 h. Cell proliferation was assessed by the BrdU incorporation assay (n = 3, *p < 0.05 vs. CT, $^{#}$p < 0.05 vs. EV$^{Cx43 +}$, §p < 0.05 vs. EV$^{Cx43 +}$ dox).

in the percentage of cells undergoing S-phase (Fig. 2c). In colony formation assays, dox-loaded EVs presented a similar effect as free dox, abolishing the clonogenic potential of 4T1^{luc2} cells (Supplementary Fig. 2c). In any circumstance, empty EVs did not present an effect. Overall, despite that no statistical significance could be achieved, dox loaded into EVs containing Cx43 presented a trend toward an enhanced anti-proliferative capacity, compared with either free dox or EV$^{Cx43 -}$ dox.

Some of these data were confirmed in another tumour cell line, MNNG/HOS, derived from an osteosarcoma. The results obtained show that metabolic activity and cell proliferation were impaired in the presence of either free or EV-dox (Supplementary Fig. 2d–f). In parallel, to attest whether this effect can be tumour specific, we evaluated the same parameters in 2 non-tumour cell lines – kidney epithelial HEK-293$^{Cx43 +}$ cells and retinal pigment epithelial Arpe-19 cells (Supplementary Fig. 3a–c). Our data show that, in this case, free dox leads to a significant decrease in the metabolic activity, BrdU incorporation and percentage of ki-67–positive cells in both non-tumour cell lines, whereas EV-dox presents minor toxicity to those cells. Altogether, the data obtained with tumoural and non-tumoural cell lines demonstrate that dox carried in EVs, compared to free dox, is more toxic to tumour cells and less toxic to non-tumour cells.

To prove that a functional channel is required to the aforementioned effects, we used a Cx43 mimetic peptide, gap26, that specifically blocks Cx43 channels (7,34). Results in Fig. 2d show that, in the presence of gap26, EV$^{Cx43 +}$ dox were no longer able to impair proliferation of recipient 4T1^{luc2} cells, whereas the use of gap26 showed no effect upon treatment with EV$^{Cx43 -}$ dox or free dox. These data provide strong evidence that the increased cytotoxicity of EV$^{Cx43 +}$ dox can be, at least partially, mediated by the function of Cx43 channels.

Furthermore, we evaluated cell motility, using time-lapse microscopy. Our results show that 4T1^{luc2} cells incubated with EV$^{Cx43 +}$ dox present a significantly reduced cell motility, compared to free dox treatment (Fig. 3a). Given that mitogen-activated protein kinases are master regulators of cell motility, survival and proliferation (35,36),
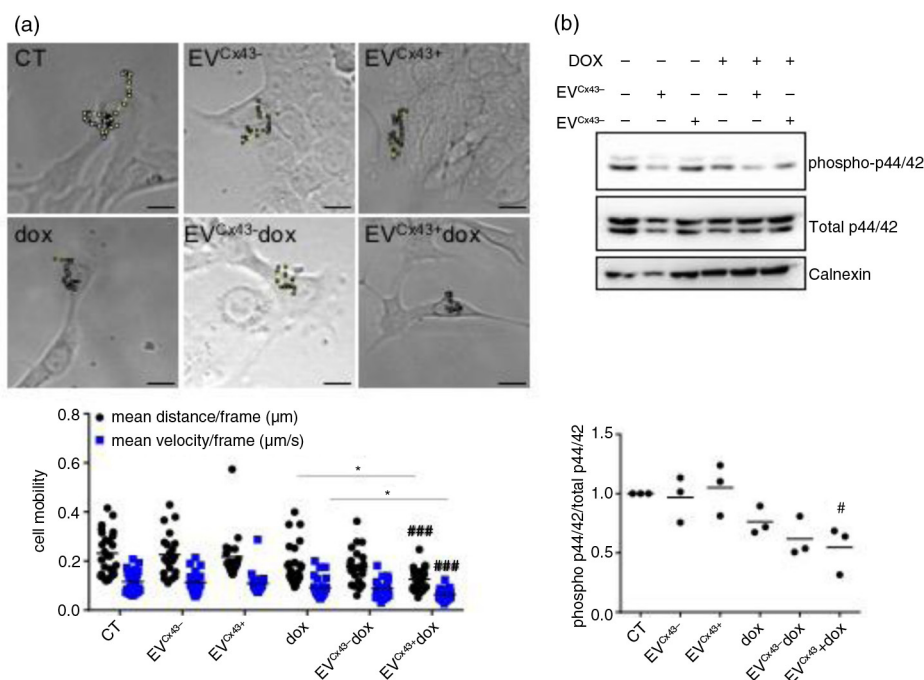
Fig. 3. Cx43-containing EVs loaded with dox decrease the activation of signalling pathways related to cell motility. The 4T1^{luc2} cells were treated with 2 µM free dox, EV^{Cx43+} dox, EV^{Cx43-} dox or vehicles, for 24 h. (a) Time-lapse microscopy was performed to assess cell motility, followed by individual cell tracking. Mean distance and velocity are plotted in the graph (n = 3, $^{###}$p < 0.001 vs. EV^{Cx43+}; *p < 0.05 EV^{Cx43+} dox vs. dox;). Left panel shows representative images of the assay. Scale bar, 10 µm. (b) Activation of the p44/42 pathway was analysed by WB. Calnexin was used as loading control (n = 3, $^{#}$p < 0.05 vs. EV^{Cx43+}).

we explored the effect of dox administration upon modulation of the p44/42 pathway. Results in Fig. 3b show a decreased activation of the p44/42 pathway in tumour cells treated with either free or EV-dox for 24 h; this decrease is only statistically significant when EV^{Cx43+} dox are used. Altogether, these data suggest that the anti-proliferative effects and disruption of cell motility in response to EV^{Cx43+} dox treatment involve a downregulation of the p44/42 pathway.

DOX loaded in EVs present therapeutic potential identical to free dox *in vivo*

Once we established the anti-tumoural effect of dox loaded in EVs *in vitro*, we proceeded to the *in vivo* studies. We started by quantitatively assessing the communication between EVs and tumour cells by using a subcutaneous mouse xenograft model with bilateral flank tumours. For that, we injected the mice i.t. with luciferin-loaded EV^{Cx43+} or EV^{Cx43-} in opposed tumours of the same animal. Results depicted in Supplementary Fig. 4 show that EV^{Cx43+} were more efficient in the delivery of luciferin to the tumours, as indicated by the 2.7-fold increase in the signal, relative to EV^{Cx43-}. Because BLI of animals receiving luciferin i.p. showed tumours with a similar signal intensity, our data support the hypothesis that the presence of Cx43 in EVs facilitates the release of intraluminal content into target tumour cells.

To investigate the therapeutic potential of Cx43-containing EVs *in vivo*, tumour-bearing mice received treatment with equal amounts of dox (0.2 mg/kg i.t.; Supplementary Fig. 5a), administered either free or encapsulated in EVs (EV^{Cx43-} dox or EV^{Cx43+} dox), 5 and 8 days post-implantation of 4T1^{luc2} cells. As controls, we used vehicle-treated animals – injected i.t. with either PBS, EV^{Cx43-} or EV^{Cx43+} at the same concentrations. Tumour response to different forms of treatment was monitored by BLI, 11 days after cell inoculation. Treatment of mice with EV^{Cx43-} dox or EV^{Cx43+} dox resulted in anti-tumoural effects similar to the free drug (Fig. 4a). In addition, we assessed tumour volumes using a manual caliper (Fig. 4b) and determined the weight of excised tumours (Fig. 4c–d). Altogether, and considering the comparison between dox-treated animals and their respective vehicles, we show that similar anti-tumoural effects were obtained for free dox and dox encapsulated in EV^{Cx43-}, whereas a better therapeutic efficiency was observed for EV^{Cx43+} dox, compared with EVs devoid of Cx43. The effect of dox-induced apoptosis was also evaluated through the analysis of Bax and Bcl2 levels in tumours after the treatments (37). Results on Fig. 4e show that only EV^{Cx43+} dox induced a statistically significant increase in the ratio Bax/Bcl2. In all the evaluated parameters, injection of empty EVs produced no effect and was therefore omitted from subsequent experiments.
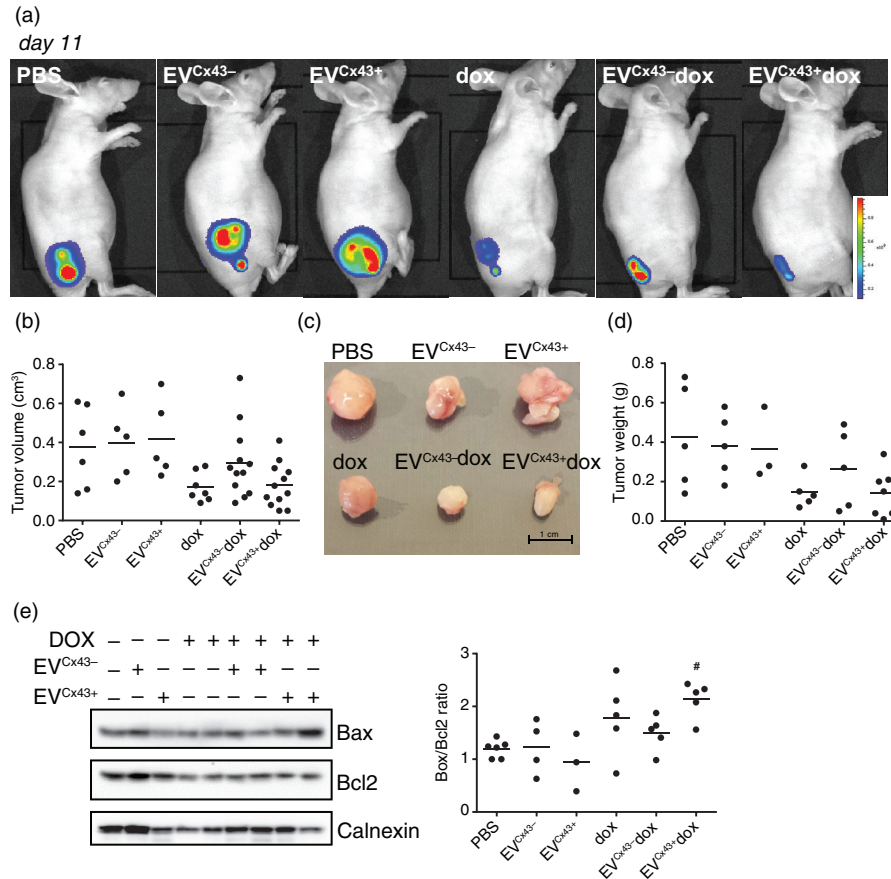
Fig. 4. EVs loaded with dox have anti-tumoural activity in 4T1^{luc2} tumour-bearing mice. Tumour-bearing mice were treated (i.t.) with 0.2 mg/kg of free dox, EV$^{Cx43 +}$dox or EV$^{Cx43 -}$dox or vehicles, on days 5 and 8 after subcutaneous inoculation of 4T1^{luc2} cells into opposed flanks. Equal amounts of EVs were used in each condition. (a) Representative BLI of mice 11 days after 4T1^{luc2} cells inoculation, corresponding to 3 days after the last treatment. (b) Tumour diameters were measured with a caliper, followed by determination of tumour volume (n = 5–8). (c) Representative images of excised tumours. (d) Average mass of excised tumours (n = 5–8). (e) WB analysis of Bax and Bcl2 in tumour lysates, for each treatment group. Ratio of Bax/Bcl2 is depicted on graph. Calnexin was used as loading control (n = 5, $^{\#}$p < 0.05 vs. EV$^{Cx43 +}$).

Herein, the term vehicle is used to designate animals that received treatment with PBS.

Subsequently, we evaluated the therapeutic value of EVs concerning the tumour growth rate, by BLI. Similar to the data presented above, dox-loaded EVs showed the same therapeutic activity as free dox, inducing a progressive decrease in tumour growth rate relative to the vehicle (Fig. 5a–b). Despite no statistical differences, a trend toward an increased efficiency for EVs containing Cx43 (comparing with EV$^{Cx43 -}$dox) was maintained. Representative images illustrating treatment with empty EVs are presented in Supplementary Fig. 5b.

Cx43-containing EVs loaded with dox ameliorate dox cardiotoxicity in vivo

Given the cardiotoxicity associated with dox-based therapies, we sought to assess whether EVs are able to mitigate such side effects in our model. To address this question, we evaluated different parameters usually implicated in dox cardiotoxicity, including oxidative stress and altered expression of cardiac-specific genes (12,27,35,36,45). Although HE staining showed no major histopathological changes, transverse diameter of the cardiomyocytes was reduced in the hearts of mice that received treatment with free dox, an effect that was prevented upon EV$^{Cx43 +}$ dox treatment (Fig. 6a, upper panel). Moreover, free dox treatment lead to increased myocardial fibrosis that was not observed in animals that received dox encapsulated in EV$^{Cx43 +}$ (Fig. 6a, bottom panel).

Dox-induced oxidative stress in the heart is mediated by the activity of COX-2, that is, the generation of reactive oxygen species responsible for the induction of small heat shock proteins (38–40). Our results show that mice treated with free dox presented increased levels of COX-2 and Hsp25 in the heart (Fig. 6b–c), whereas in those mice that received dox encapsulated in Cx43-containing EVs, the cardiac levels of these proteins remained unaltered.
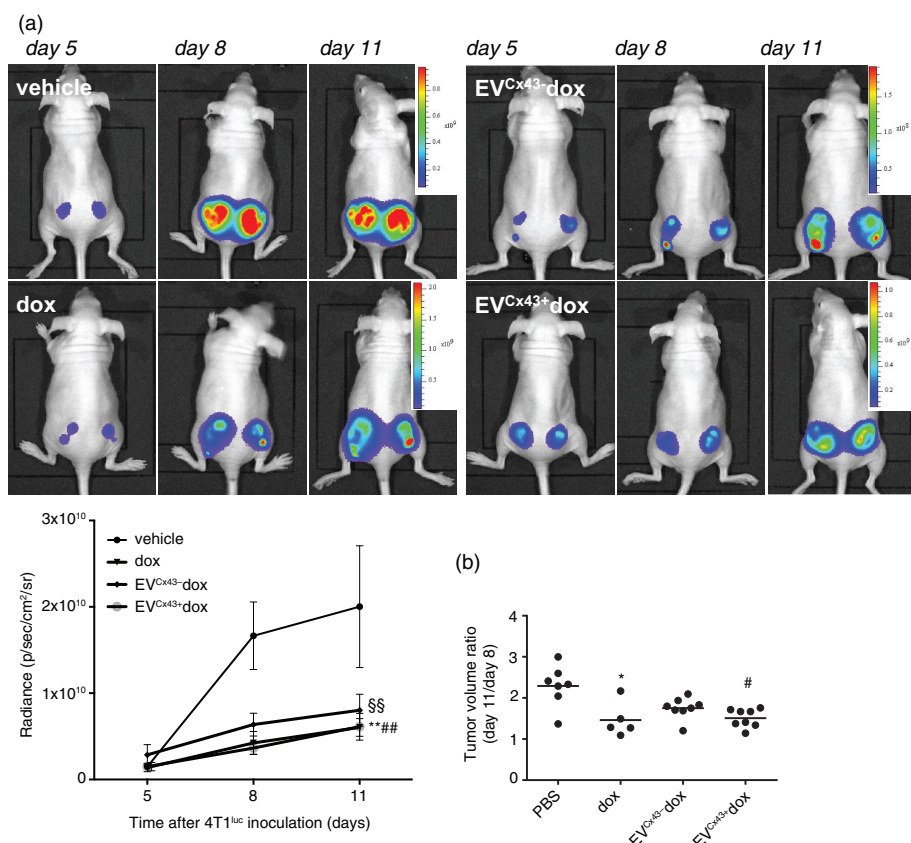
(a)

Fig. 5. EVs loaded with dox inhibit tumour growth *in vivo*. Representative serial BLI of mice bearing bilateral 4T1^{luc2} subcutaneous tumours before treatment (at day 5), and at days 8 and 11 after cells inoculation, corresponding to 3 days after the first and second treatments, respectively. Treatment groups received (i.t.) 0.2 mg/kg of free dox, EV$^{Cx43 -}$ dox or EV$^{Cx43 +}$ dox, on days 5 and 8. Equal amounts of EVs were used in each condition. (a) Tumour size was evaluated by quantification of bioluminescence signal (p/sec/cm^2/sr) in a ROI drawn around the tumour. Graph depicts tumour progression of untreated and treated animals, normalized to the signal at the beginning of the treatment (n = 5, **p < 0.01 dox vs. vehicle, §§p < 0.01 EV$^{Cx43 +}$ dox vs. vehicle, $^{##}$p < 0.05 EV$^{Cx43 +}$ vs. vehicle). (b) Tumour diameters were measured to calculate tumour volume ratio between days 11 and 8 (n = 5–8, *p < 0.05 vs. vehicle, $^#$p < 0.05 vs. vehicle).

Several cardiomyopathies have been associated with GJ remodelling, which is accompanied by alterations of the levels and/or subcellular distribution of Cx43, the more abundant GJ protein in the myocardium (28,41). Results depicted in Fig. 6d show that free dox lead to a marked increase in the levels of Cx43 in the heart, which was prevented by EV$^{Cx43 +}$ dox treatment. Concerning the animals treated with EV$^{Cx43 -}$ dox, they presented an intermediate phenotype, with an upregulation of COX-2 and Cx43, but not of Hsp25, and induction of fibrosis.

Altogether, these results demonstrate that i.t. administration of dox causes morphological and molecular alterations in the heart that can partially be attenuated using EV$^{Cx43 +}$ as a delivery vehicle of dox.

Discussion

It has become increasingly evident that EVs are major conveyors of biological information between cells, making them appealing candidates for directed drug delivery.

Although various studies have shown that these endogenous vesicles can be used to deliver therapeutic cargo to specific tissues (46), we are still far from reaching the standardization needed to translate those evidences into the clinical arena. Indeed, many drawbacks, including some lack of specificity of EV to desirable target cells, causing adverse effects, have hampered the enthusiasm around of EV-based therapeutics. Therefore, the development of strategies that aim to improve the efficacy of using EVs as drug delivery systems with decreased side effects are vital to boost this highly promising field of research. In the present report, we show that EVs can be successfully used to deliver dox to tumour cells *in vitro* and *in vivo*, rendering a similar chemotherapeutic effect to that of the free drug. More importantly, we demonstrate that the presence of Cx43 in EVs potentially increases the therapeutic value of these vesicles by reducing the cardiotoxicity of dox.

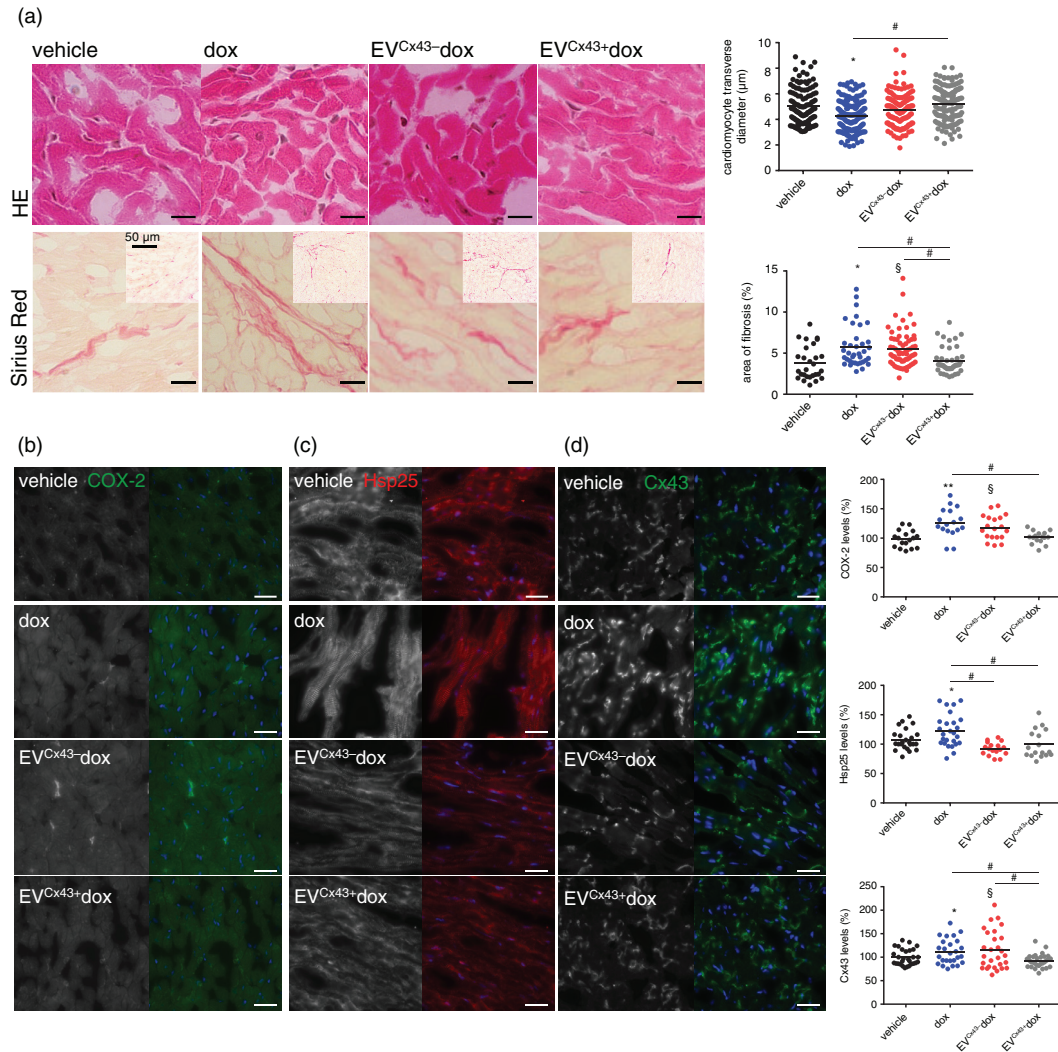Despite the theoretical high potential of EVs as dox vehicles for anti-tumour therapy, only 1 study from Tian

Fig. 6. Cx43-containing EVs ameliorate dox cardiotoxicity *in vivo*. Tumour-bearing mice were treated (i.t.) with 0.2 mg/kg of free dox, $EV^{Cx43 +}$ dox or $EV^{Cx43 -}$ dox 5 and 8 days after bilateral subcutaneous 4T1^{luc2} cells inoculation. At day 11, mice were sacrificed and hearts were collected. (a) Histological analysis of hearts was performed by HE and Sirius red staining. Scale bars, 5 μm. Insets represent low-magnification images. Quantitative measurements obtained in each field analysed by microscopy are depicted in the graph (n = 3–4, *p < 0.05 dox vs. vehicle; §p < 0.05 $EV^{Cx43 -}$ dox vs. vehicle; #p < 0.05). Expression of COX-2 (green) (b) Hsp25 (red) (c) and Cx43 (green) (d) was assessed by immunofluorescence. Nuclei were stained with Dapi. Scale bars, 20 μm. Graphs depict quantification of each individual field analysed by fluorescence microscopy (n = 3–4, *p < 0.05, **p < 0.01 dox vs. vehicle; §p < 0.05 $EV^{Cx43 -}$ dox vs. vehicle; #p < 0.05).

et al. has shown that exogenous loading of dox into exosomes can be used to inhibit tumour growth, using a breast cancer mice model (10,40). Therefore, the results gathered in our report constitute an important step forward in favour of EVs as suitable delivery vehicles. In addition, we provided important insights regarding the mechanisms whereby dox-loaded EVs exert therapeutic effects, showing that EV-dox impair metabolic activity and proliferation of tumour cells *in vitro*, cause cell cycle arrest and impair clonogenic ability of 4T1^{luc2} cells.

Concerning the donor cell type for vesicle production, we used EVs from HEK-293 cells. HEK-293 cells have

been shown to be suitable for the delivery of other therapeutic compounds in different animal models of disease, including models of cancer and hepatic disorders (10,11).

The more challenging step of targeted drug delivery is still the design of vesicles with enhanced tropism to tumour cells. For example, Ohno et al. demonstrated that the miRNA let-7A can be successfully delivered by exosomes displaying an epidermal growth factor receptor ligand, leading to growth inhibition of breast cancer xenografts (4). It was also demonstrated that the presence of iRGD peptides at the exosomal surface increase the efficiency of

dox delivery to tumour cells by targeting upregulated integrin receptors, with a concomitant decrease of toxicity to non-target organs (10). Because the expression of Cx43 in tumour and stromal cells can correlate with the malignancy and metastatic potential of tumours (42), it is conceivable that Cx43 constitutes a suitable target to direct therapeutic vesicles, within specific types and/or stages of tumour development. In the present study, we show that the presence of Cx43 in EVs increases the delivery efficiency of small compounds, such as luciferin, into luciferase-expressing tumour cells, *in vitro* and *in vivo*. Although the presence of Cx43 in EVs did not show a statistically significant difference in terms of therapeutic effect of dox, in the majority of the evaluated parameters there is a clear trend for $EV^{Cx43\,+}$ to present a better anti-tumoural performance, compared to $EV^{Cx43\,-}$.

Moreover, the fact that the specific hemichannel inhibitor gap26 was able to prevent the effect of $EV^{Cx43\,+}$ dox on cell proliferation impairment, underpins our model in which functional Cx43 channels are required for the cytotoxicity of $EV^{Cx43\,+}$ dox. This lead us to propose that, in addition to endocytosis and membrane fusion of EVs with recipient cells, an alternative and/or complementary mechanism, involving the docking of Cx43 channels present in both EVs and cells, can contribute for a more efficient and/or rapid communication between recipient cells and EVs (43). This can be relevant, for example, to bypass inflammasome activation or rapid lysosomal degradation of intraluminal cargo, thus improving the value of EVs as therapeutic carriers (3).

In line with a previous study (13), our data show that cardiac damage, induced by treatment of tumour-bearing mice with free dox (i.t.), including morphological alterations, increased fibrosis and upregulation of oxidative stress response, can be attenuated when dox is carried by Cx43-containing EVs, whereas delivery through $EV^{Cx43\,-}$ did not ameliorate dox cardiotoxicity. Given that in physiological conditions, in the heart, Cx43 is mainly present at the intercalated discs, forming GJ, these fully assembled channels would not be available to dock with Cx43 channels present at the EV membranes, which could, at least partially, explain our results. In contrast, EVs devoid of Cx43 would be preferentially taken up by endocytosis and/or fusion, still causing some degree of toxicity to the heart. Alternatively, it is plausible that Cx43-containing EVs can be retained in other organs and do not reach the heart.

In agreement with a recent report (44), we found that free dox lead to an upregulation of Cx43, an effect that is absent from hearts of animals treated with $EV^{Cx43\,+}$ dox. Although in our study, we did not explore in detail the subcellular distribution of cardiac Cx43, it is conceivable that after dox exposure Cx43 accumulates at the intercalated discs, thus accounting for an increased intercellular communication that could have a detrimental effect not only through alterations to the electrical conduction system

required for synchronous heart contraction, but also by contributions to the spread of damage signals, which, in this case, would exacerbate dox-induced cardiotoxicity.

Overall, our results constitute an important contribution to reinforce the emerging and very promising idea that EVs constitute an efficient drug delivery vehicle for anti-tumoural therapeutic approaches. Moreover, we provide strong evidence that the presence of Cx43 in dox-containing EVs can reduce cardiotoxicity, without compromising its therapeutic efficiency.

Authors' contributions

HG coordinated the study, designed experiments, analysed data and wrote the manuscript. TMM designed and performed the experiments, discussed the data and wrote the manuscript. CG designed and performed the experiments and discussed the data. MJP performed the experiments. MZ performed the TEM experiments. CO, JPGS and PP contributed to the writing and revision of the manuscript.

Conflict of interest and funding

References

1. Kourembanas S. Exosomes: vehicles of intercellular signaling, biomarkers, and vectors of cell therapy. Annu Rev Physiol. 2015;77:13–27.
2. Gould SJ, Raposo G. As we wait: coping with an imperfect nomenclature for extracellular vesicles. J Extracell Vesicles. 2013;2:20389, doi: http://dx.doi.org/10.3402/jev.v2i0.20389
3. György B, Hung ME, Breakefield XO, Leonard JN. Therapeutic applications of extracellular vesicles: clinical promise and open questions. Annu Rev Pharmacol Toxicol. 2015;55:439–64.
4. Ohno S, Takanashi M, Sudo K, Ueda S, Ishikawa A, Matsuyama N, et al. Systemically injected exosomes targeted to EGFR deliver antitumor microRNA to breast cancer cells. Mol Ther. 2013;21:185–91.
5. Tickner JA, Urquhart AJ, Stephenson S-A, Richard DJ, O'Byrne KJ. Functions and therapeutic roles of exosomes in cancer. Front Oncol. 2014;4:127.

6. Mulcahy LA, Pink RC, Carter DRF. Routes and mechanisms of extracellular vesicle uptake. J Extracell Vesicles. 2014;3: 24641, doi: http://dx.doi.org/10.3402/jev.v3.24641

7. Soares AR, Martins-Marques T, Ribeiro-Rodrigues T, Ferreira JV, Catarino S, Pinho MJ, et al. Gap junctional protein Cx43 is involved in the communication between extracellular vesicles and mammalian cells. Sci Rep. 2015;5:13243.

8. Zhuang X, Xiang X, Grizzle W, Sun D, Zhang S, Axtell RC, et al. Treatment of brain inflammatory diseases by delivering exosome encapsulated anti-inflammatory drugs from the nasal region to the brain. Mol Ther. 2011;19:1769–79.

9. Mizrak A, Bolukbasi MF, Ozdener GB, Brenner GJ, Madlener S, Erkan EP, et al. Genetically engineered microvesicles carrying suicide mRNA/Protein inhibit schwannoma tumor growth. Mol Ther. 2013;21:101–8.

10. Tian Y, Li S, Song J, Ji T, Zhu M, Anderson GJ, et al. A doxorubicin delivery platform using engineered natural membrane vesicle exosomes for targeted tumor therapy. Biomaterials. 2014;35:2383–90.

11. Johnsen KB, Gudbergsson JM, Skov MN, Pilgaard L, Moos T, Duroux M. A comprehensive overview of exosomes as drug delivery vehicles – endogenous nanocarriers for targeted cancer therapy. Biochim Biophys Acta. 2014;1846:75–87.

12. Ewer MS, Ewer SM. Cardiotoxicity of anticancer treatments. Nat Rev Cardiol. 2015;12:547–58.

13. Toffoli G, Hadla M, Corona G, Caligiuri I, Palazzolo S, Semeraro S, et al. Exosomal doxorubicin reduces the cardiac toxicity of doxorubicin. Nanomedicine (Lond). 2015 [cited 2016 May 5]. Available from: http://www.ncbi.nlm.nih.gov/pubmed/26420143

14. Lener T, Gioma M, Aigner L, Börger V, Buzas E, Camussi G, et al. Applying extracellular vesicles based therapeutics in clinical trials – an ISEV position paper. J Extracell Vesicles. 2015;4:30087, doi: http://dx.doi.org/10.3402/jev.v4.30087

15. Elzarrad MK, Haroon A, Willecke K, Dobrowolski R, Gillespie MN, Al-Mehdi A-B, et al. Connexin-43 upregulation in micrometastases and tumor vasculature and its role in tumor cell attachment to pulmonary endothelium. BMC Med. 2008;6:20.

16. McLachlan E, Shao Q, Laird DW. Connexins and gap junctions in mammary gland development and breast cancer progression. J Membr Biol. 2007;218:107–21.

17. Ferreira-Teixeira M, Parada B, Rodrigues-Santos P, Alves V, Ramalho JS, Caramelo F, et al. Functional and molecular characterization of cancer stem-like cells in bladder cancer: a potential signature for muscle-invasive tumors. Oncotarget. 2015;6:36185–201.

18. Martins-Neves SR, Paiva-Oliveira DI, Wijers-Koster PM, Abrunhosa AJ, Fontes-Ribeiro C, Bovée JVMG, et al. Chemotherapy induces stemness in osteosarcoma cells through activation of Wnt/β-catenin signaling. Cancer Lett. 2016; 370:286–95.

19. Lim E, Modi KD, Kim J. *In vivo* bioluminescent imaging of mammary tumors using IVIS spectrum. J Vis Exp. 2009. pii: 1210. [cited 2016 May 4]. Available from: http://www.ncbi.nlm.nih.gov/pubmed/19404236

20. Théry C, Amigorena S, Raposo G, Clayton A, Théry C, Amigorena S, et al. Isolation and characterization of exosomes from cell culture supernatants and biological fluids. In: Current protocols in cell biology. Hoboken, NJ: Wiley; 2006. p. 3.22.1–3.22.29. [cited 4 May 2016]. Available from: http://doi.wiley.com/10.1002/0471143030.cb0322s30

21. Montecalvo A, Larregina AT, Shufesky WJ, Stolz DB, Sullivan MLG, Karlsson JM, et al. Mechanism of transfer of functional microRNAs between mouse dendritic cells via exosomes. Blood. 2012;119:756–66.

22. Johnson S, Nguyen V, Coder D, Johnson S, Nguyen V, Coder D. Assessment of cell viability. In: Current protocols in cytometry. Hoboken, NJ: Wiley; 2013. p. 9.2.1–9.2.26. [cited 2016 Jun 6]. Available from: http://doi.wiley.com/10.1002/0471142956.cy0902s64

23. Strober W. Trypan blue exclusion test of cell viability. In: Current protocols in immunology. Hoboken, NJ: Wiley; 2015. p. A3.B.1–A3.B.3. [cited 2016 Jun 6]. Available from: http://doi.wiley.com/10.1002/0471142735.ima03bs111

24. Butler M, Spearman M, Braasch K. Monitoring cell growth, viability, and apoptosis. Methods Mol Biol. 2014;1104:169–92.

25. Pozarowski P, Darzynkiewicz Z. Analysis of cell cycle by flow cytometry. In: Checkpoint controls and cancer. Totowa, NJ: Humana Press. p. 301–12. [cited 2016 May 5]. Available from: http://link.springer.com/10.1385/1-59259-811-0:301

26. Jain P, Worthylake RA, Alahari SK. Quantitative analysis of random migration of cells using time-lapse video microscopy. J Vis Exp. 2012;63:e3585.

27. Franken NAP, Rodermond HM, Stap J, Haveman J, van Bree C. Clonogenic assay of cells *in vitro*. Nat Protoc. 2006;1: 2315–9.

28. Martins-Marques T, Catarino S, Zuzarte M, Marques C, Matafome P, Pereira P, et al. Ischemia-induced autophagy leads to degradation of gap junction protein connexin43 in cardiomyocytes. Biochem J. 2015;467:231–45.

29. Martins-Marques T, Catarino S, Marques C, Matafome P, Ribeiro-Rodrigues T, Baptista R, et al. Heart ischemia results in connexin43 ubiquitination localized at the intercalated discs. Biochimie. 2015;112:196–201.

30. Kawaguchi T, Takemura G, Kanamori H, Takeyama T, Watanabe T, Morishita K, et al. Prior starvation mitigates acute doxorubicin cardiotoxicity through restoration of autophagy in affected cardiomyocytes. Cardiovasc Res. 2012; 96:456–65.

31. Weissgerber TL, Milic NM, Winham SJ, Garovic VD, Cooper R, Schriger D, et al. Beyond bar and line graphs: time for a new data presentation paradigm. PLoS Biol. 2015;13: e1002128.

32. Lötvall J, Hill AF, Hochberg F, Buzás EI, Vizio D Di, Gardiner C, et al. Minimal experimental requirements for definition of extracellular vesicles and their functions: a position statement from the International Society for Extracellular Vesicles. J Extracell Vesicles. 2014;3:26913, doi: http://dx.doi.org/10.3402/jev.v3.26913

33. Hanahan D, Weinberg RA. Hallmarks of cancer: the next generation. Cell. 2011;144:646–74.

34. Hawat G, Benderdour M, Rousseau G, Baroudi G. Connexin 43 mimetic peptide Gap26 confers protection to intact heart against myocardial ischemia injury. Pflugers Arch. 2010;460: 583–92.

35. Vial E, Sahai E, Marshall CJ. ERK-MAPK signaling coordinately regulates activity of Rac1 and RhoA for tumor cell motility. Cancer Cell. 2003;4:67–79.

36. Zhang W, Liu HT. MAPK signal pathways in the regulation of cell proliferation in mammalian cells. Cell Res. 2002;12:9–18.

37. Chen GG, Lai PBS, Hu X, Lam IKY, Chak ECW, Chun YS, et al. Negative correlation between the ratio of Bax to Bcl-2 and the size of tumor treated by culture supernatants from Kupffer cells. Clin Exp Metastasis. 2002;19:457–64.

38. Octavia Y, Tocchetti CG, Gabrielson KL, Janssens S, Crijns HJ, Moens AL. Doxorubicin-induced cardiomyopathy: from molecular mechanisms to therapeutic strategies. J Mol Cell Cardiol. 2012;52:1213–25.

39. Vedam K, Nishijima Y, Druhan LJ, Khan M, Moldovan NI, Zweier JL, et al. Role of heat shock factor-1 activation in the

doxorubicin-induced heart failure in mice. Am J Physiol Heart Circ Physiol. 2010;298:H1832–41.

40. Dowd NP, Scully M, Adderley SR, Cunningham AJ, Fitzgerald DJ. Inhibition of cyclooxygenase-2 aggravates doxorubicin-mediated cardiac injury *in vivo*. J Clin Invest. 2001;108:585–90.

41. Martins-Marques T, Catarino S, Marques C, Pereira P, Girão H. To beat or not to beat: degradation of Cx43 imposes the heart rhythm. Biochem Soc Trans. 2015;43:476–81.

42. Radić J, Krušlin B, Šamija M, Ulamec M, Milošević M, Jazvić M, et al. Connexin 43 expression in primary colorectal carcinomas in patients with Stage III and IV disease. Anticancer Res. 2016;36:2189–96.

43. Colombo M, Raposo G, Théry C. Biogenesis, secretion, and intercellular interactions of exosomes and other extracellular vesicles. Annu Rev Cell Dev Biol. 2014;30:255–89.

44. Pecoraro M, Sorrentino R, Franceschelli S, Del Pizzo M, Pinto A, Popolo A. Doxorubicin-mediated cardiotoxicity: role of mitochondrial connexin 43. Cardiovasc Toxicol. 15: 366–76.

45. Zhang X, Teodoro JG, Nadeau JL. Intratumoral gold-doxorubicin is effective in treating melanoma in mice. Nanomedicine. 2015;11:1365–75.

46. Tang K, Zhang Y, Zhang H, Xu P, Liu J, Ma J, et al. Delivery of chemotherapeutic drugs in tumour cell-derived microparticles. Nat Commun. 2012;3:1282.